PROCEEDINGS OF SCIENCE

Photon–photon fusion measurements at ATLAS

Samira Hassani[*†]
IRFU, CEA, Université Paris-Saclay, Gif-sur-Yvette; France.
E-mail: samira.hassani@cea.fr

Photon-photon fusion is a rare process at hadron and ion colliders. It is particularly interesting as a remarkably clean interaction with little (if any) remnant activity from the interacting particles. In this talk we present the status of photon-photon fusion measurements with the ATLAS detector. The observation of light-by-light scattering and the measurement of dimuon pairs in ultraperipheral Pb+Pb collisions are presented. The potential of axion-like particle searches with the upgraded ATLAS detector in Large Hadron Collider Runs 3 and 4 is reported. Intact protons from the photon-photon fusion process are scattered at small angles in diffractive and electromagnetic processes, and the protons are tagged by the ATLAS Forward Proton (AFP) detectors. These detectors can operate during standard high-luminosity LHC runs and collect data corresponding to a large integrated luminosity. The AFP detectors and their tracking performance during 2017 and 2018 operations are presented.

XXVII International Workshop on Deep-Inelastic Scattering and Related Subjects - DIS2019
8-12 April, 2019
Torino, Italy

[*]Speaker.
[†]On behalf of the ATLAS Collaboration.

PoS(DIS2019)055

1. Observation of light-by-light scattering in ultraperipheral Pb+Pb collisions

Light-by-light (LbyL) scattering, $\gamma\gamma \to \gamma\gamma$, is a quantum-mechanical process that is forbidden in the classical theory of electrodynamics [1]. In the standard model (SM), the $\gamma\gamma \to \gamma\gamma$ reaction proceeds at lowest order in the fine structure constant ($\alpha_{\rm em}$) via virtual one-loop box diagrams involving charged fermions (leptons and quarks) and the $W^{\pm}$ boson. However, in various extensions of the SM, extra contributions are possible, making the measurement of LbyL scattering sensitive to new physics. The relevant examples are the axion-like particles (ALPs) and higher-dimension operators. LbyL interactions can also occur in relativistic heavy-ion collisions at large impact parameters, i.e. larger than twice the radius of the ions. The strong interaction does not play a role in these ultra-peripheral collision (UPC) events. The electromagnetic (EM) fields produced by the colliding Pb nuclei can be treated as a beam of quasi-real photons with a small virtuality of $Q^2 < 1/R^2$, where R is the radius of the charge distribution and so $Q^2 < 10^{-3}$ GeV^2. Then, the cross section for the reaction Pb+Pb$(\gamma\gamma) \to$ Pb+Pb$\,\gamma\gamma$ can be calculated by convolving the respective photon flux with the elementary cross section for the process $\gamma\gamma \to \gamma\gamma$. Since the photon flux associated with each nucleus scales as Z^2, the cross section is extremely enhanced as compared to proton–proton (pp) collisions. Evidence for this process in PbPb UPC at the Large Hadron Collider (LHC) has been reported by the ATLAS [2] and CMS [3] collaborations, based on the PbPb dataset of 0.4 nb^{-1} recorded in 2015 at a centre-of-mass energy of $\sqrt{s} = 5.02$ TeV.

The ATLAS Collaboration has reported recently the observation of $\gamma\gamma \to \gamma\gamma$ scattering with a significance beyond 8 standard deviations [4] in PbPb collisions at $\sqrt{s} = 5.02$ TeV. The analysis is performed using a data sample corresponding to an integrated luminosity of 1.73 nb^{-1}, collected in November 2018 by the ATLAS experiment [5] at the LHC. Candidate diphoton events are recorded using a dedicated trigger for events with moderate activity in the calorimeter but little additional activity in the detector. Light-by-light scattering event candidates are selected in events with two photons produced exclusively, each with transverse energy $E_{\rm T}^{\gamma} > 3$ GeV and pseudorapidity $|\eta_{\gamma}| < 2.37$ and diphoton invariant mass $m_{\gamma\gamma}$ above 6 GeV. Backgrounds can come mainly from the central exclusive production of two photons from the fusion of two gluons (CEP $gg \to \gamma\gamma$), as well as from misidentified electrons from the $\gamma\gamma \to ee$ process. The background contribution from $gg \to q\bar{q}$ production is estimated using MC simulation and is found to be negligible. To reduce other fake-photon backgrounds, such as cosmic-ray muons, the transverse momentum of the diphoton system ($p_{\rm T}^{\gamma\gamma}$) is required to be below 1 GeV for $m_{\gamma\gamma} < 12$ GeV and below 2 GeV for $m_{\gamma\gamma} > 12$ GeV. To reduce prompt-photon background from CEP $gg \to \gamma\gamma$ reactions, an additional requirement on the reduced acoplanarity, Aco $= (1 - |\Delta\phi_{\gamma\gamma}|/\pi) < 0.01$, is used. The above requirements define the fiducial region for the signal measurement.

The $\gamma\gamma \to ee$ yield in the signal region is evaluated using a data-driven method. Two control regions are defined with exactly two photons passing the signal selection, but requiring also one or two associated pixel tracks. The event yield observed in these two control regions is extrapolated to the signal region using the probability to miss the electron pixel track if the electron track is not reconstructed. The CEP contribution is evaluated from a control region defined by applying the same selection as for the signal region, but inverting the Aco requirement to Aco > 0.01 (see Fig-

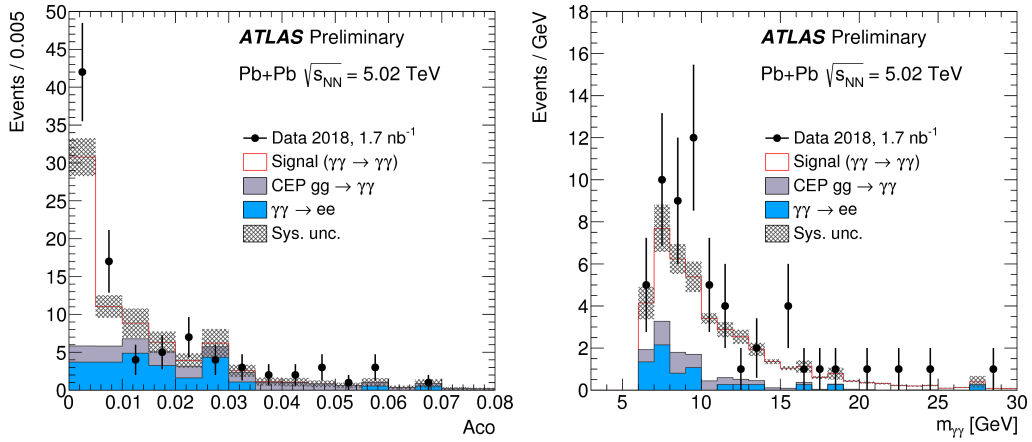

Figure 1: The diphoton reduced acoplanarity distribution for events satisfying the signal selection, but before the Aco < 0.01 requirement (left). Diphoton invariant mass for events satisfying the signal selection (right) [4].

ure 1), and correcting the measured event yield for the expected signal and $\gamma\gamma \to ee$ contributions. After applying all selection criteria, 59 candidate events are observed for a background expectation of 12 ± 3 events. The diphoton invariant mass distribution for events satisfying all selection criteria is shown in Figure 1. An excess of events over the expected background is found with an observed significance of 8.2 standard deviations.

The cross section for the $\gamma\gamma \to \gamma\gamma$ process is measured in a fiducial phase space, defined by a set of requirements on the diphoton final state, reflecting the selection at reconstruction level described above. The measured fiducial cross section is $\sigma_{\text{fid}} = 79 \pm 13$ (stat.) ± 7 (syst.) ± 3 (lumi.) nb. The overall uncertainty is dominated by uncertainties in the photon reconstruction efficiency (4%) and the trigger efficiency (2%). The measured fiducial cross section can be compared with the predicted values of 45 ± 5 nb from Ref. [6], 51 ± 5 nb from Ref. [7] and 50 ± 5 nb from SuperChic3 MC simulation [12]. The experiment-to-prediction ratios are 1.73 ± 0.40, 1.53 ± 0.33 and 1.56 ± 0.33, respectively.

2. Potential of ALP searches in UPC interactions with the upgraded ATLAS detector in LHC Runs 3 and 4

The potential of ALP searches in UPC Pb+Pb collisions is studied using the upgraded ATLAS detector with an expected integrated luminosity of 10 nb^{-1} delivered in LHC Runs 3 and 4 [9]. The photon-ALP interaction can be described by a Lagrangian density of the form: $\mathscr{L}_{a\gamma\gamma} = \frac{1}{4\Lambda} a F^{\mu\nu} \tilde{F}_{\mu\nu}$, where a is the massive scalar ALP field (of mass m_a) and $1/\Lambda$ is the coupling of the interaction (the dimension of Λ is energy). The result is obtained using reconstructed-level quantities with the selection requirements described in Section 1. In addition to these selection criteria, and in order to increase the sensitivity to the ALP signal, a requirement of $p_{\text{T}}^{\gamma\gamma}/m_{\gamma\gamma} > 0.35$ is applied. The invariant mass distribution is used as the discriminating variable, with bin widths comparable to the expected resolution of a narrow resonant signal. A binned likelihood function is constructed in each

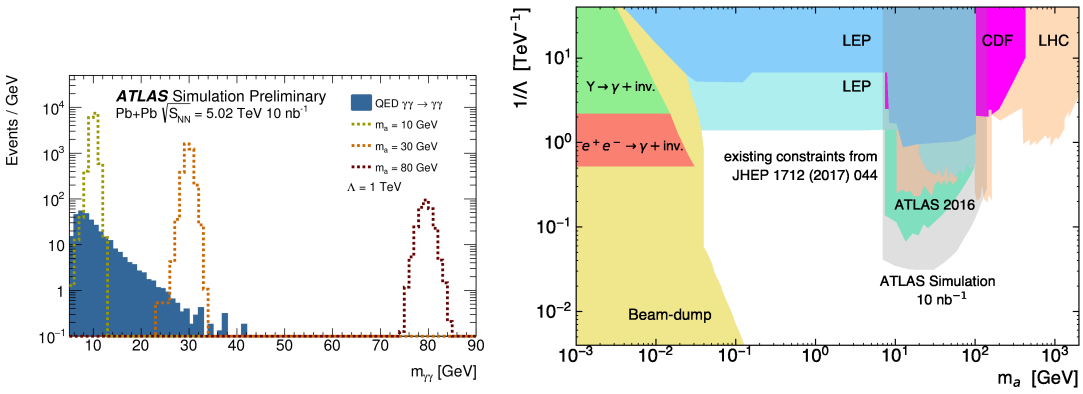

Figure 2: Diphoton invariant mass distribution shown for three different values of axion-like particle signal: $m_{\mathrm{a}} = 10, 30, 80$ GeV (left). Upper limits on the coupling $(1/\Lambda)$ as a function of the ALP mass (right). A compilation of exclusion limits obtained by different experiments is also shown [9].

bin of the diphoton $m_{\gamma\gamma}$ distribution from the Poisson probability of the sum of the contributions of the background and of a hypothetical signal of strength relative to the benchmark model. This likelihood function is used to set limits on the presence of a signal. In Figure 2 the expected mass distributions for three ALP signal mass values and the main background from the $\gamma\gamma \to \gamma\gamma$ process are shown. In this study, other sources of backgrounds are neglected, since they have been found to be small. Upper limits are set on the product of the production cross section of new resonances and their decay branching ratio into $\gamma\gamma$ and is then translated into a limit on the coupling $(1/\Lambda)$, as presented in Figure 2.

3. Measurement of high-mass dimuon pairs

Exclusive dimuon production ($\gamma\gamma \to \mu^+\mu^-$) in ultra-peripheral Pb+Pb collisions is measured for dimuon invariant masses $m_{\mu\mu} > 10$ GeV and pair rapidity $|Y_{\mu\mu}| < 2.4$ [10]. The events are selected using a single-muon trigger with a little additional activity in the detector. The events are required to have a primary vertex formed from two oppositely-charged muons, each having transverse momentum $p_{\mathrm{T}}^{\mu} > 4$ GeV and pseudorapidity $|\eta_{\mu}| < 2.4$. The distributions are all corrected for trigger efficiency, reconstruction efficiency, and vertex reconstruction efficiency.
Cross sections as a function of dimuon pair mass and pair rapidity are shown in Figure 3. The results are compared with the STARLIGHT 1.1 [11] Monte Carlo, which incorporates calculations of the photon flux from each nucleus and leading-order QED cross sections. The simulations are in reasonable agreement with the measured cross sections, suggesting that the nuclear electromagnetic fields are reasonably described by the equivalent photon approximation and that the nuclear form factor is adequately implemented in STARLIGHT.

4. ATLAS Forward Proton Detectors

The ATLAS Forward Proton (AFP) detector [13] provides measurements of the momentum and emission angle of very forward protons. This enables the observation and measurement of a

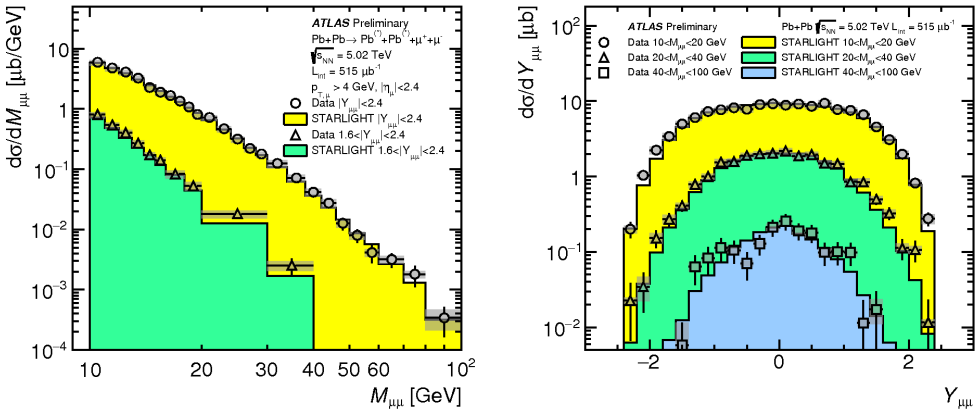

Figure 3: Cross section for dimuon production in ultra-peripheral Pb+Pb collisions, as a function of dimuon pair mass (left) and pair rapidity (right) [10].

range of processes where one or both protons remain intact in pp collisions. Such processes are associated with elastic and diffractive scattering. The AFP consists of two Roman Pot (RP) stations (called Near and Far) on each side of ATLAS. They are located about 210 m from the ATLAS Interaction Point and can be inserted horizontally into the LHC beam pipe in the immediate vicinity of the beams. Each RP consists of four Silicon Tracker planes. Additionally, Far stations host the Time of Flight detectors.

In 2017 the full system was installed: two arms with two stations in each. During standard and special runs 32 fb^{-1} of data were recorded. The AFP tracking performance are studied. The efficiency was measured for the three different occupancy regions with different track multiplicities as a function of the bias voltage. Tracks are reconstructed using three planes, and extrapolated to the fourth plane. The extrapolated position is compared to the hit position in the fourth plane as shown in Figure 4. The track reconstruction requires a single cluster per plane, consisting of no more than two pixels. In Figure 4, the efficiency is shown for the three different occupancy regions with different track multiplicities as a function of the bias voltage. The occupancy regions are defined as high (above 70%), medium (between 30 and 70%) and low (below 30%). Full efficiency is recovered for all the regions for a bias voltage larger than 30V.

References

[1] W. Heisenberg and H. Euler. Folgerungen aus der Diracschen Theorie des Positrons. *Z. Phys.*, 98(11):714–732, 1936.

[2] ATLAS Collaboration. Evidence for light-by-light scattering in heavy-ion collisions with the ATLAS detector at the LHC. *Nature Phys.*, 13(9):852–858, 2017.

[3] CMS Collaboration. Evidence for light-by-light scattering and searches for axion-like particles in ultraperipheral PbPb collisions at $\sqrt{s_{\rm NN}} = 5.02$ TeV. (arXiv:1810.04602. CMS-FSQ-16-012-004).

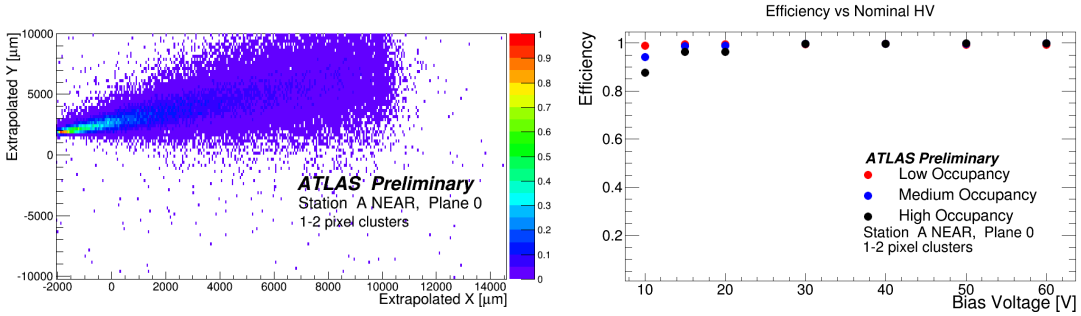

Figure 4: Extrapolated position in Plane 0 using the track reconstructed by planes 1,2 and 3 (left). AFP efficiency as a function of bias voltage for three different occupancies (right) [14].

[4] ATLAS Collaboration. Observation of light-by-light scattering in ultraperipheral Pb+Pb collisions with the ATLAS detector. (arXiv:1904.03536).

[5] ATLAS Collaboration. The ATLAS experiment at the CERN Large Hadron Collider. *JINST*, 3:S08003, 2008.

[6] David d'Enterria and Gustavo G. da Silveira. Observing Light-by-Light Scattering at the Large Hadron Collider. *Phys. Rev. Lett.*, 111:080405, 2013. [Erratum: Phys. Rev. Lett. **116** (2016) 129901].

[7] Mariola Klusek-Gawenda, Piotr Lebiedowicz, and Antoni Szczurek. Light-by-light scattering in ultraperipheral Pb-Pb collisions at energies available at the CERN Large Hadron Collider. *Phys. Rev. C*, 93(4):044907, 2016.

[8] L. A. Harland-Lang, V. A. Khoze, and M. G. Ryskin. Exclusive LHC physics with heavy ions: SuperChic 3. *Eur. Phys. J. C*, 79(1):39, 2019.

[9] Prospects for Measurements of Photon-Induced Processes in Ultra-Peripheral Collisions of Heavy Ions with the ATLAS Detector in the LHC Runs 3 and 4. Technical Report ATL-PHYS-PUB-2018-018, CERN, Geneva, Oct 2018. http://cds.cern.ch/record/2641655.

[10] Measurement of high-mass dimuon pairs from ultraperipheral lead-lead collisions at $\sqrt{s_{\mathrm{NN}}} = 5.02$ TeV with the ATLAS detector at the LHC. Technical Report ATLAS-CONF-2016-025, CERN, Geneva. http://cds.cern.ch/record/2157689.

[11] Spencer R. Klein, Joakim Nystrand, Janet Seger, Yuri Gorbunov, and Joey Butterworth. STARlight: A Monte Carlo simulation program for ultra-peripheral collisions of relativistic ions. *Comput. Phys. Commun.*, 212:258–268, 2017.

[12] L. A. Harland-Lang, V. A. Khoze, and M. G. Ryskin. Exclusive LHC physics with heavy ions: SuperChic 3. *Eur. Phys. J. C*, 79(1):39, 2019.

[13] L Adamczyk, E Bana, A Brandt, M Bruschi, S Grinstein, J Lange, M Rijssenbeek, P Sicho, R Staszewski, T Sykora, M Trzebiski, J Chwastowski, and K Korcyl. Technical Design Report for the ATLAS Forward Proton Detector. Technical Report CERN-LHCC-2015-009. ATLAS-TDR-024. http://cds.cern.ch/record/2017378.

[14] Chiara Grieco. ATLAS Forward Proton Detector. Technical Report ATL-FWD-PROC-2018-005, CERN, Geneva. https://cds.cern.ch/record/2640536.